

# Towards Trustworthy Multimodal Recommendation

Zixuan Li

Renmin University of China  
Haidian Qu, Beijing Shi, China

## Abstract

Recent advances in multimodal recommendation have demonstrated the effectiveness of incorporating visual and textual content into collaborative filtering. However, real-world deployments raise an increasingly important yet underexplored issue: trustworthiness. On modern e-commerce platforms, multimodal content can be misleading or unreliable (e.g., visually inconsistent product images or click-bait titles), injecting untrustworthy signals into multimodal representations and making existing multimodal recommenders brittle under modality corruption. In this work, we take a step towards trustworthy multimodal recommendation from both a method and an analysis perspective. First, we propose a plug-and-play modality-level rectification component that mitigates untrustworthy modality features by learning soft correspondences between items and multimodal features. Using lightweight projections and Sinkhorn-based soft matching, the rectification suppresses mismatched modality signals while preserving semantically consistent information, and can be integrated into existing multimodal recommenders without architectural modifications. Second, we present two practical insights on interaction-level trustworthiness under noisy collaborative signals: (i) training-set pseudo interactions can help or hurt performance under noise depending on prior-signal alignment; and (ii) propagation-graph pseudo edges can also help or hurt robustness, as message passing may amplify misalignment. These findings highlight that graph enrichment strategies driven by collaborative priors are not universally beneficial under untrustworthy interactions, and that trustworthy multimodal recommendation requires careful handling of both content and interaction signals. Extensive experiments on multiple datasets and backbones under varying corruption levels demonstrate improved robustness from modality rectification and validate the above interaction-level observations.

## CCS Concepts

- Information systems → Recommender systems; Multimedia and multimodal retrieval.

## Keywords

Multimodal Recommendation, Trustworthy Recommendation, Graph Refinement, Graph Neural Networks, Multimodal Consistency

## 1 Introduction

In the era of information explosion, Recommender Systems (RS) have become a pivotal technology for alleviating information overload by analyzing historical user behaviors to provide personalized suggestions [1, 15–17]. However, traditional Collaborative Filtering (CF) algorithms, which rely exclusively on user-item interaction history, often suffer from severe data sparsity, limiting recommendation accuracy and coverage[3, 10, 14, 18]. To address this limitation,

**Multimodal Recommender Systems (MRSs)** have emerged by integrating rich item content—such as product images and textual descriptions—to enhance user preference modeling, especially for sparse and cold-start items[20, 31, 36, 38, 39].

Along this line, multimodal recommendation has evolved from simple feature fusion to graph-based modeling. Early methods (e.g., VBPR [6], DeepStyle [21]) project visual or textual features into low-dimensional spaces and combine them with ID embeddings. More recent approaches employ lightweight graph message passing (e.g., LightGCN [7]) to capture high-order collaborative signals, and further exploit modality-induced item relations via similarity graphs (e.g., LATTICE [34]). Several works also study robustness via interaction-graph refinement or modality-noise suppression (e.g., FREEDOM [38], MGNC [32], SMORE [12], PGL [33]). Despite these advances, a common but implicit assumption is that multimodal content is reliable and that observed interactions faithfully reflect user preference. This assumption is increasingly violated in real-world platforms, where item content can be misleading yet plausible (e.g., image–text mismatch, click-bait titles) and implicit feedback can include unreliable interactions (e.g., misclicks or exposure-driven behaviors). We refer to this practical challenge as the **trustworthiness** issue in multimodal recommendation: the reliability of multimodal signals and interaction edges for preference learning may vary substantially, and such inconsistencies can be amplified by graph propagation and even confound common training/evaluation practices, rather than behaving as random feature perturbations.

To illustrate the problem, we present a case study based on the Amazon Baby dataset (Figure 1). First, the product image shows a children’s friendship bracelet craft kit, while the textual description discusses baby milestone onesie stickers, resulting in a severe semantic inconsistency between visual and textual modalities. Such misleading-yet-plausible content is common on real-world platforms and can induce erroneous cross-modal correlations when models treat all modalities as equally reliable. Second, the same figure shows a user interaction set dominated by maternal and infant products with highly consistent functionality and usage scenarios (e.g., bathtub, infant rocker, and cradle swing), while also containing a product (e.g., a reusable wet bag) that exhibits weak semantic relevance to the user’s primary interests. This suggests that untrustworthy interactions exist in implicit-feedback logs: weakly related but plausible clicks/purchases can be indiscriminately propagated during message passing, thereby polluting collaborative signals. These observations motivate studying trustworthy multimodal recommendation from two perspectives: (i) content trust, i.e., rectifying misleading modality signals at the feature level, and (ii) interaction trust, i.e., understanding when graph-based enhancement may amplify unreliable collaborative relations.

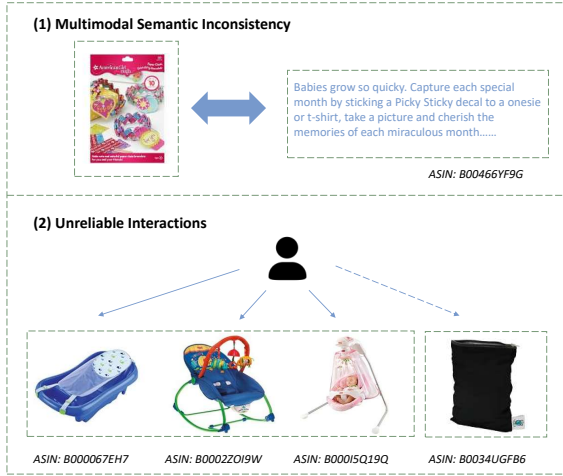


**Figure 1: Illustration of untrustworthy signals in multimodal recommendation. (1) Multimodal semantic inconsistency between product images and textual descriptions. (2) Unreliable user–item interactions, where weakly related but plausible interactions introduce low-confidence edges that may pollute message passing.**

To this end, we propose a simple, plug-and-play modality-level rectification component that can be integrated into existing multimodal recommenders without architectural changes. The key idea is to learn soft correspondences between items and multimodal features, emphasizing semantically consistent signals while down-weighting mismatched ones. We instantiate it with a lightweight projection and Sinkhorn-based soft matching, yielding a principled and stable correspondence approximation under modality mismatch.

Beyond this component, we conduct an interaction-level trustworthiness analysis and derive two practical insights. (**Insight 1**) Under corrupted collaborative signals, injecting pseudo interactions (e.g., from collaborative priors or augmentation) into the training set is a double-edged sword: it can help when injected priors align with true patterns, but degrade robustness when misaligned, even with strict validation/test exclusion. (**Insight 2**) Injecting pseudo edges only into the propagation graph can likewise help or hurt; in particular, message passing may amplify misaligned relations and reduce robustness. Overall, generated interactions should be used cautiously, and their integration with graph propagation should be carefully controlled when interaction trustworthiness is low.

The primary contributions are summarized as follows:

- **Trustworthiness in Multimodal Recommendation.** We identify and formulate trustworthiness failures in MRSs arising from misleading multimodal content and unreliable implicit interactions, and instantiate them with reproducible controlled stress tests.
- **Modality-level Rectification.** We propose a plug-and-play module that learns item–modality soft correspondences via lightweight projection and Sinkhorn-based matching,

suppressing mismatched signals while preserving consistent semantics.

- **Interaction-level Insights.** We show that training-time pseudo interactions and propagation-time pseudo edges are not universally beneficial under corrupted collaborative signals: they can help or harm depending on prior–signal alignment, and propagation may amplify misaligned relations.
- **Effectiveness and Generality.** Experiments across multiple datasets and backbones demonstrate improved robustness under modality corruption and validate the above interaction-level insights under noisy interactions.

## 2 Related Work

**Multimodal Recommendation.** Multimodal recommendation augments collaborative signals with item-side content such as images and texts to mitigate interaction sparsity and improve preference estimation[6, 9, 11, 35]. Early multimodal recommenders typically injected visual (and/or textual) features extracted by pretrained encoders into matrix-factorization-style ranking objectives. For instance, VBPR [6] extends BPR [14] by incorporating visual features into personalized ranking, while DeepStyle [21] explores leveraging deep visual representations for style-aware recommendation. These methods are conceptually simple and effective, yet they largely model multimodal content as static side information and have limited ability to exploit high-order user–item connectivity.

More recent work has shifted toward graph-based multimodal modeling, motivated by the success of message passing in graph collaborative filtering [7, 24, 30]. A representative line builds multimodal graph neural recommenders that propagate signals on the interaction graph while fusing multi-view (ID/content) item representations, such as MMGCN [25], DualGNN [22], and Multi-View GCN variants [2, 32, 36]. Beyond directly applying message passing on the observed user–item graph, several studies explicitly model item–item relations derived from multimodal similarity. LATTICE [34] introduces latent structure learning to construct and leverage item graphs induced by multimodal features, thereby enriching item affinity beyond co-interactions. However, learning and updating such structures can be computationally costly. FREEDOM [38] revisits this design by decoupling relatively stable item relations from noisy interactions: it freezes the (static) item graph and focuses on refining the user–item interaction graph, improving practicality for large-scale training[26].

Robustness has also become an explicit objective in multimodal recommendation. MGNC [32] leverages behavioral signals to purify multimodal features by filtering preference-irrelevant components. BM3 [39] studies self-supervised bootstrapping for better generalization, while SMORE [12], PGL [33], and related methods focus on modality fusion and noise suppression from frequency-structure-aware perspectives. Despite these advances, most multimodal recommenders still implicitly assume that multimodal content is trustworthy and that noise mainly stems from stochastic perturbations. In practice, however, platforms often contain misleading-yet-plausible content (e.g., image–text mismatch, click-bait descriptions) and unreliable implicit interactions, which can systematically bias representation learning beyond random noise [5, 23, 31]. This

motivates studying trustworthiness from both content and interaction perspectives: rectifying semantic pollution in multimodal features, and examining when graph-based enhancement may amplify untrustworthy collaborative signals. In particular, we analyze collaborative-prior-guided graph enhancement (e.g., GraphDA [5]-like strategies) and show its effects can be non-monotonic under corrupted collaborative signals—helpful when priors align with true patterns but harmful when misaligned due to error amplification in message passing.

*Noisy Correspondence and Multimodal Mismatch.* Beyond feature perturbations, a growing line of multimodal learning research studies noisy correspondence, where paired samples across modalities are partially mismatched (false positives/negatives), which can severely harm cross-modal alignment [8, 27, 28]. Representative methods estimate soft correspondence targets or enforce consistency regularization to down-weight mismatched pairs, e.g., BiCro [28] and ESC [29], and robust contrastive learning further mitigates noisy views/false positives in self-supervised objectives [4]. While these techniques are primarily developed for contrastive alignment and retrieval objectives, they motivate a key principle relevant to multimodal recommendation: correspondence between item-level modalities can be unreliable and should be softly rectified rather than treated as clean pairs. Following this principle, we design a lightweight correspondence-based rectification that is compatible with pairwise ranking objectives and can be plugged into diverse recommenders with negligible overhead.

### 3 Preliminaries

*Setting and notation.* We study implicit-feedback multimodal recommendation. Let  $\mathcal{U} = \{u_1, \dots, u_M\}$  and  $\mathcal{I} = \{i_1, \dots, i_N\}$  denote the user and item sets, respectively. Observed interactions form a binary matrix  $\mathbf{Y} \in \{0, 1\}^{M \times N}$ , where  $y_{ui} = 1$  indicates an interaction (e.g., click/purchase). Equivalently, we denote the observed positive edge set as  $\mathcal{E}^+ = \{(u, i) \mid y_{ui} = 1\}$  and the user–item bipartite graph as  $\mathcal{G} = (\mathcal{U} \cup \mathcal{I}, \mathcal{E}^+)$ . Each item  $i$  is associated with pre-extracted multimodal features  $\tilde{\mathbf{e}}_i^m \in \mathbb{R}^{d_m}$  for modality  $m \in \mathcal{M}$ . In this work,  $\mathcal{M} = \{v, t\}$  (image/text) with  $d_v = 4096$  and  $d_t = 384$ .

*Recommendation objective.* Given  $\mathcal{G}$  and  $\{\tilde{\mathbf{e}}_i^m\}$ , a multimodal recommender learns a scoring function  $\hat{y}_{ui}$  for top- $K$  ranking. All backbones considered in our experiments are optimized with the standard BPR objective with uniform negative sampling:

$$\mathcal{L}_{\text{BPR}} = \sum_{(u, i, j)} -\log \sigma(\hat{y}_{ui} - \hat{y}_{uj}) + \Omega_{\text{backbone}}, \quad (1)$$

where  $(u, i) \in \mathcal{E}^+$  and  $j$  is uniformly sampled from items not interacted by  $u$ , and  $\Omega_{\text{backbone}}$  denotes backbone-specific regularizers/auxiliary losses. In all experiments, we keep each backbone’s original objective and tuned hyperparameters unchanged.

*Trustworthiness-aware corruptions.* We consider two practical sources of untrustworthiness and simulate them in controlled settings.

**(1) Modality misalignment (feature-level corruption).** A fraction of item-side modality features can be semantically mismatched (e.g., wrong image/title). To simulate this, for each modality  $m \in \mathcal{M}$  and a corruption ratio  $\eta_m \in [0, 0.5]$ , we uniformly

sample a subset  $\mathcal{S}_m \subseteq \mathcal{I}$  with  $|\mathcal{S}_m| = \lfloor \eta_m |\mathcal{I}| \rfloor$  and randomly permute modality features within  $\mathcal{S}_m$ :

$$\{\tilde{\mathbf{e}}_i^m\}_{i \in \mathcal{S}_m} \leftarrow \text{Permute}(\{\tilde{\mathbf{e}}_i^m\}_{i \in \mathcal{S}_m}). \quad (2)$$

Image and text corruptions are applied independently, and all random seeds are fixed for reproducibility. Unless stated otherwise, in this setting we treat the observed interaction graph  $\mathcal{G}$  as reliable and focus on rectifying feature-level untrustworthiness.

**(2) Interaction noise (graph-level corruption).** Observed interactions may contain spurious edges or miss meaningful ones. We simulate graph-level corruption by randomly editing the training edges with a noise ratio  $\eta_e$ . Specifically, edge deletion removes  $\lfloor \eta_e |\mathcal{E}^+| \rfloor$  edges uniformly at random from  $\mathcal{E}^+$ , while edge addition uniformly samples the same number of non-existing user–item pairs  $(u, i) \notin \mathcal{E}^+$  and adds them as positive training edges. All random seeds are fixed. Note that these add/delete operations are solely used to simulate interaction noise; our interaction-level analyses in Section 5 further study how injecting edges into the training set versus the propagation graph affects robustness under such noise.

## 4 Methodology

### 4.1 Backbone Multimodal Recommender

We consider a general multimodal recommendation setting with an observed user–item interaction graph  $\mathcal{G}$  and item-side multimodal features  $\{\tilde{\mathbf{e}}_i^m\}_{m \in \mathcal{M}}$  (e.g., image/text), where  $\tilde{\mathbf{e}}_i^m \in \mathbb{R}^{d_m}$  denotes the observed feature of modality  $m$  for item  $i$ . A multimodal backbone predicts a preference score  $\hat{y}_{ui}$  for each user–item pair, which we abstract as a scoring function

$$\hat{y}_{ui} = f_\theta(u, i; \mathcal{G}, \{\tilde{\mathbf{e}}_i^m\}_{m \in \mathcal{M}}), \quad (3)$$

where  $\theta$  denotes backbone parameters.

*Offline plug-and-play integration.* Our Modality-level Rectification Module is applied offline as a preprocessing step: it takes the observed (potentially misaligned) modality features  $\{\tilde{\mathbf{e}}_i^m\}$  and outputs rectified features  $\{\mathbf{e}_i^{m,\text{rect}}\}$  with the same dimensionality as the original inputs. We then fix  $\{\mathbf{e}_i^{m,\text{rect}}\}$  and train the backbone with its original objective without architectural modification, by directly replacing the modality inputs:

$$f_\theta(u, i; \mathcal{G}, \{\tilde{\mathbf{e}}_i^m\}) \Rightarrow f_\theta(u, i; \mathcal{G}, \{\mathbf{e}_i^{m,\text{rect}}\}). \quad (4)$$

In this work, we evaluate this integration on three representative multimodal recommenders, including LATTICE, FREEDOM, MGNC, SMORE and VBPR by only replacing their modality inputs with fixed  $\mathbf{e}_i^{m,\text{rect}}$  while keeping architectures and objectives unchanged.

### 4.2 Modality-level Rectification Module

In real-world e-commerce, the modality signal attached to an item may be misaligned with the item semantics (e.g., wrong images or misleading titles), which violates the one-to-one correspondence assumption between items and their multimodal content. Following our trustworthiness-aware formulation, we model such feature-level untrustworthiness as an unreliable item–modality association (i.e., the observed modality feature of item  $i$  may originate from another item). To rectify misaligned modality features in a plug-and-play manner, we propose a **Modality-level Rectification Module**

that learns soft correspondences between items and modality signals and then uses the correspondences to re-aggregate modality features.

*Anchor embeddings.* The key idea is to introduce a comparatively reliable anchor representation for each item and align multimodal signals to this anchor space. In the modality-untrustworthy setting studied in this section, we assume the observed user-item interactions are reliable, while the multimodal features may be misaligned. Accordingly, we obtain the anchor by pre-training a LightGCN encoder on the observed interaction graph and use its collaborative item embedding as the anchor:

$$\mathbf{e}_i = \frac{1}{L+1} \sum_{\ell=0}^L \mathbf{e}_i^{(\ell)}. \quad (5)$$

We then  $\ell_2$ -normalize the anchor as  $\tilde{\mathbf{e}}_i = \mathbf{e}_i / \|\mathbf{e}_i\|$ .

*Step 1: Robust modality-to-anchor projection.* Given the observed modality feature  $\tilde{\mathbf{e}}_i^m \in \mathbb{R}^{d_m}$  for modality  $m \in \mathcal{M}$ , we learn a light-weight projection

$$\mathbf{z}_i^m = g_m(\tilde{\mathbf{e}}_i^m) \in \mathbb{R}^d, \quad (6)$$

where  $g_m(\cdot)$  is implemented as a linear layer. We normalize projected vectors as  $\tilde{\mathbf{z}}_i^m = \mathbf{z}_i^m / \|\mathbf{z}_i^m\|$  and adopt a cosine regression objective:

$$\ell_i^m = 1 - \langle \tilde{\mathbf{e}}_i, \tilde{\mathbf{z}}_i^m \rangle. \quad (7)$$

Since a fraction of observed pairs  $(i, \tilde{\mathbf{e}}_i^m)$  can be mismatched, directly minimizing the average loss is sensitive. We thus employ a small-loss selection strategy: within each mini-batch, we keep only the lowest-loss (highest-similarity) subset and optimize their average:

$$\mathcal{L}_{\text{proj}}^m = \frac{1}{|\mathcal{B}_{\text{keep}}|} \sum_{i \in \mathcal{B}_{\text{keep}}} \ell_i^m, \quad (8)$$

where  $\mathcal{B}_{\text{keep}}$  keeps a fixed ratio  $\rho$  of the smallest-loss instances in the batch. This yields a robust projection that is less affected by mismatched item-modality pairs.

*Step 2: Sparse affinity construction.* After obtaining projected modality representations, we estimate soft correspondences between anchors and modality signals across all items. We first compute the cosine similarity matrix

$$s_{ij}^m = \langle \tilde{\mathbf{e}}_i, \tilde{\mathbf{z}}_j^m \rangle, \quad (9)$$

and then build a sparse affinity matrix  $\mathbf{A}^m \in \mathbb{R}_+^{N \times N}$  by keeping only the top- $K$  neighbors for each anchor:

$$\mathbf{A}_{ij}^m = \begin{cases} \exp(s_{ij}^m / \tau), & j \in \text{TopK}_K(\{s_{ij}^m\}_{j=1}^N), \\ 0, & \text{otherwise,} \end{cases} \quad (10)$$

where  $\tau$  is a temperature hyper-parameter. To avoid over-correction, we enforce that the diagonal entry  $\mathbf{A}_{ii}^m$  is included in the sparse candidates.

*Step 3: Sinkhorn-based soft matching.* A row-normalized affinity may suffer from “hubness” (a few modality signals attract too many anchors). To obtain a more balanced correspondence that approximates a soft one-to-one assignment, we apply a Sinkhorn-Knopp scaling procedure on  $\mathbf{A}^m$  and obtain a soft matching matrix  $\mathbf{P}^m$ :

$$\mathbf{P}^m = \text{diag}(\mathbf{u}) \mathbf{A}^m \text{diag}(\mathbf{v}), \quad (11)$$

where  $\mathbf{u}, \mathbf{v} \in \mathbb{R}_+^N$  are iteratively updated to make  $\mathbf{P}^m$  approximately doubly-stochastic (i.e., row/column sums close to constants):

$$\mathbf{u} \leftarrow \mathbf{1} \oslash (\mathbf{A}^m \mathbf{v} + \epsilon), \quad \mathbf{v} \leftarrow \mathbf{1} \oslash ((\mathbf{A}^m)^\top \mathbf{u} + \epsilon), \quad (12)$$

with  $\oslash$  denoting element-wise division. We implement the above procedure on sparse matrices to keep the complexity linear in the number of non-zeros ( $\mathcal{O}(NK)$ ) and we run Sinkhorn iterations with a small  $\epsilon$  for numerical stability.

*Step 4: Feature rectification via correspondence aggregation.* Given the soft matching matrix  $\mathbf{P}^m$ , we rectify the raw modality features by aggregating signals from matched items:

$$\hat{\mathbf{e}}_i^m = \sum_{j=1}^N \mathbf{P}_{ij}^m \tilde{\mathbf{e}}_j^m. \quad (13)$$

Finally, we adopt a diagonal prior mix to preserve part of the original observation and avoid aggressive replacement:

$$\mathbf{e}_i^{m,\text{rect}} = \lambda \tilde{\mathbf{e}}_i^m + (1 - \lambda) \hat{\mathbf{e}}_i^m, \quad (14)$$

where  $\lambda \in [0, 1]$  controls the strength of rectification.

## 5 Interaction-level Trustworthiness Insights

Real-world implicit-feedback graphs are often untrustworthy: observed interactions may contain spurious edges (e.g., misclicks or exposure-driven behaviors) and miss meaningful ones. A common practice to mitigate such noise is to edit the interaction graph using a collaborative prior (e.g., add “high-confidence” edges or prune “low-confidence” ones). In this section, we examine this practice under controlled stress tests and show that similarity-based edge editing is not universally beneficial under noisy interactions: it can help or hurt depending on the noise type and the reliability (alignment) of the collaborative prior.

### 5.1 Stress-test Setting

We simulate untrustworthy interactions by randomly corrupting the training edge set  $\mathcal{E}_{\text{tr}}^+$  with a noise ratio  $\eta_e$  (Sec. 3): we either (i) delete a fraction of training edges, or (ii) add the same number of random non-existing user-item pairs as positive training edges. This random add/delete is only used to construct noisy training data for stress testing; the edge editing strategy studied below is fully similarity-based and contains no random edge generation.

### 5.2 Similarity-based Edge Editing with a Collaborative Prior

**5.2.1 Collaborative prior and similarity.** Given a (possibly noisy) training graph, we pre-train a LightGCN encoder on the corrupted  $\mathcal{E}_{\text{tr}}^+$  and obtain user/item embeddings  $\mathbf{e}_u, \mathbf{e}_i$ . We define the collaborative similarity as

$$s_{ui} = \mathbf{e}_u^\top \mathbf{e}_i. \quad (15)$$

We then study two widely-used graph editing operations separately: **edge pruning** and **relation completion**. Importantly, both operations are rank-based and control the final number of edited edges with a fixed ratio  $r$ . Specifically, we set  $r = 5\%$  to control the editing magnitude. Pruning always removes exactly  $r|\mathcal{E}_{\text{tr}}^+|$  edges, while completion attempts to add  $r|\mathcal{E}_{\text{tr}}^+|$  candidate edges and may end up with fewer after holdout filtering.

### 5.2.2 Editing operations.

*Edge pruning (similarity-based deletion).* To remove potentially spurious interactions, we delete the bottom- $r\%$  observed training edges according to  $s_{ui}$ :

$$\mathcal{E}_{\text{tr}}^{\text{prune}} = \mathcal{E}_{\text{tr}}^+ \setminus \text{Bottom}_r(\{s_{ui} \mid (u, i) \in \mathcal{E}_{\text{tr}}^+\}), \quad (16)$$

where  $\text{Bottom}_r(\cdot)$  selects the subset of observed edges whose similarities fall into the lowest  $r\%$  among all training positives.

*Relation completion (similarity-based addition).* To recover potentially missing relations, we first generate high-confidence candidates from both user and item sides using top- $K$  selection:

$$\mathcal{N}_U(u) = \text{TopK}_{K_{UI}^{(u)}}(\{i \in \mathcal{I} \mid (u, i) \notin \mathcal{E}_{\text{tr}}^+\}, s_{ui}), \quad (17)$$

$$\mathcal{N}_I(i) = \text{TopK}_{K_{UI}^{(i)}}(\{u \in \mathcal{U} \mid (u, i) \notin \mathcal{E}_{\text{tr}}^+\}, s_{ui}), \quad (18)$$

and take the union as the candidate set

$$C_{\text{tr}} = \{(u, i) \mid i \in \mathcal{N}_U(u)\} \cup \{(u, i) \mid u \in \mathcal{N}_I(i)\}. \quad (19)$$

We then add the top- $r\%$  edges in  $C_{\text{tr}}$  by similarity, yielding

$$\mathcal{E}_{\text{tr}}^{\text{comp}} = \mathcal{E}_{\text{tr}}^+ \cup \text{Top}_r(\{s_{ui} \mid (u, i) \in C_{\text{tr}}\}), \quad (20)$$

where  $\text{Top}_r(\cdot)$  selects the subset of candidate edges whose similarities fall into the highest  $r\%$  among all candidates. To avoid any information leakage, we further remove from the added edges those appearing in validation/test splits; therefore the final number of added edges is at most  $r|\mathcal{E}_{\text{tr}}^+|$  and can be smaller, i.e.,

$$|\mathcal{E}_{\text{tr}}^{\text{comp}}| \leq (1+r)|\mathcal{E}_{\text{tr}}^+|. \quad (21)$$

**5.2.3 Where to apply editing: supervision vs. propagation.** We further distinguish where to apply edge editing in graph-based recommenders. Let  $\mathcal{E}_{\text{tr}}^+$  denote the edge set used to form BPR training triplets (i.e., the supervision signal), and let  $\mathcal{E}_{\text{prop}}$  denote the edge set used for message passing. We consider three variants: (TRAIN-ONLY) edit  $\mathcal{E}_{\text{tr}}^+$  but keep  $\mathcal{E}_{\text{prop}}$  unchanged; (GRAPH-ONLY) edit  $\mathcal{E}_{\text{prop}}$  but keep  $\mathcal{E}_{\text{tr}}^+$  unchanged; (BOTH) edit both. These variants share the same backbone and objective; only the edge sets used for supervision and/or propagation differ.

## 5.3 Key Findings and Practical Takeaways

*Key findings and explanations.* Across varying interaction-noise ratios, we observe non-monotonic effects of similarity-based completion and pruning (Sec. 6.5). **When there is no interaction noise**, the LightGCN prior is generally reliable, and both completion and pruning are typically beneficial. **When noise is injected**, the effectiveness of edge editing becomes unstable and can help or hurt depending on the noise type and the resulting prior-signal alignment. In particular, under random edge additions, the learned similarity  $s_{ui}$  is often contaminated, so the gains from completion/pruning often diminish and the base model can become competitive or even preferable. Under random edge deletions, the collaborative prior can be sometimes useful and sometimes misleading: LightGCN may recover meaningful structure and benefit from completion/pruning in some cases, but may also mis-rank edges and degrade performance in others. **Completion can hurt** because  $s_{ui}$  learned from noisy interactions may be biased; adding “high-similarity” edges may introduce additional false positives into supervision and/or propagation. **Pruning can hurt** because a

**Table 1: Dataset Statistics**

Dataset	#User	#Item	#Interaction	Sparsity
Baby	19,445	7,050	160,792	99.883%
Sports	35,598	18,357	296,337	99.955%
Electronics	192,403	63,001	1,689,188	99.986%

noisy prior may mis-rank true preference edges, and deleting low-similarity edges may remove rare but informative signals in sparse graphs. Moreover, GRAPH-ONLY editing may amplify misaligned neighbors through multi-hop message passing, while TRAIN-ONLY editing directly perturbs supervision via label editing; applying edits to BOTH can compound these effects. Overall, these results caution against treating collaborative-prior-based edge editing as a universal remedy for noisy implicit feedback, and motivate validating such edits under stress tests.

*Practical takeaways. (Evaluation caveat under filtering).* In implicit-feedback evaluation, it is common to filter training positives from the candidate set when computing Recall/NDCG. Therefore, TRAIN-ONLY and BOTH edge editing (label editing) changes the set of filtered items: deleting training positives reduces the filtered set and can make evaluation scores appear artificially higher, even when true preference learning does not improve. To ensure fair comparison, filtering should be performed w.r.t. the original training positives before editing, or results should be reported under consistent candidate sets.

*(When denoising can backfire).* Our results suggest that collaborative-prior-based edge editing is not a universal remedy under noisy interactions: editing supervision perturbs the learning signal, while editing the propagation graph can amplify erroneous neighbors through message passing. In practice, edge editing should be validated under stress tests; when interaction trustworthiness is low or the prior is unstable, it can be safer to decouple editing from propagation or apply conservative edits.

## 6 Experiments

### 6.1 Experimental Setup

**6.1.1 Datasets.** Following prior multimodal recommendation works, we conduct experiments on three Amazon Review subsets: *Baby*, *Sports and Outdoors*, and *Electronics* (denoted as *Baby*, *Sports*, and *Electronics*). We apply the standard 5-core preprocessing on both users and items, and report statistics in Table 1. For the visual modality, we use 4,096-dimensional VGG16 features [19]. For the textual modality, we use sentence-transformers [13] to encode the concatenation of brand, title, description, and category into a 384-dimensional embedding.

**6.1.2 Backbones and Integration.** We evaluate representative multimodal recommenders as backbones, covering both MF-style and graph-based paradigms: **VBPR**, **LATTICE**, **FREEDOM**, **SMORE**, and **MGCN**. Our modality-level rectification is an offline preprocessing step that replaces the original modality features  $\{\tilde{\mathbf{e}}_i^m\}$  with rectified features  $\{\mathbf{e}_i^{m,\text{rect}}\}$ , while keeping each backbone’s original architecture, objective, and tuned hyperparameters unchanged.

We additionally study interaction-level edge editing under noisy interactions, which applies only to message-passing graph-based backbones.

**6.1.3 Evaluation Protocol.** We follow standard protocols in multimodal recommendation. User-item interactions are split into 80%/10%/10% for training/validation/testing. Hyperparameters are tuned on validation and all results are reported on the test set. We adopt full-ranking evaluation, where each user ranks all candidate items, and report Recall@ $K$  and NDCG@ $K$  averaged over test users. For all edge-editing variants, we perform filtering w.r.t. the original training positives (before editing) to ensure a consistent candidate set.

**6.1.4 Implementation Details.** All methods are implemented in the MMrec framework [37] with a fixed random seed. We use batch size 2048 for training and 4096 for evaluation. Models are trained for up to 1000 epochs with early stopping (patience 30 on validation Recall@10). Parameters are initialized with Xavier and optimized with Adam (default settings unless specified).

The projection step adopts small-loss selection with keep ratio  $\rho$ . In controlled modality-misalignment stress tests, we set  $\rho = \eta_m + 0.05$ , where  $\eta_m$  is the injected misalignment ratio and 0.05 approximates inherent misalignment in raw data. In practice,  $\rho$  can be chosen via a lightweight estimate of the misalignment rate (e.g., random auditing of image-text pairs or simple consistency checks).

## 6.2 Modality-level Rectification: Clean Performance

Table 2 reports the clean-setting performance of five multimodal recommenders (VBPR, LATTICE, MGNC, FREEDOM, and SMORE) on three datasets (Baby, Sports, and Electronics). We denote our Modality-level Rectification as **MR** and integrate it offline by directly replacing the original modality features with rectified ones while keeping each backbone’s architecture, objective (including backbone-specific losses/regularizers), and tuned hyperparameters unchanged. For each metric, we bold the better result between the backbone and its **+MR** variant.

**MR is non-invasive on clean inputs and often yields consistent gains.** Overall, adding **MR** does not degrade clean performance and frequently brings noticeable improvements across datasets and backbones. On Baby, **+MR** improves all GNN-based backbones (LATTICE/MGNC/FREEDOM/SMORE) consistently on both Recall and NDCG metrics, while VBPR remains essentially unchanged on R@10 and shows a small gain on NDCG. On Sports, **+MR** improves VBPR and the stronger GNN-based backbones (FREEDOM/SMORE) in most metrics, with only marginal differences for some model-metric pairs (e.g., LATTICE and MGNC). On Electronics, **+MR** again yields consistent improvements for VBPR, FREEDOM, and SMORE across all four metrics, while MGNC is largely unchanged.

**Discussion: why can MR help even without corruption?** Although MR is designed for modality misalignment, the clean-setting gains suggest that real-world multimodal features may still contain mild noise or semantic inconsistency. By learning soft item-modality correspondences and applying a conservative diagonal-prior mix,

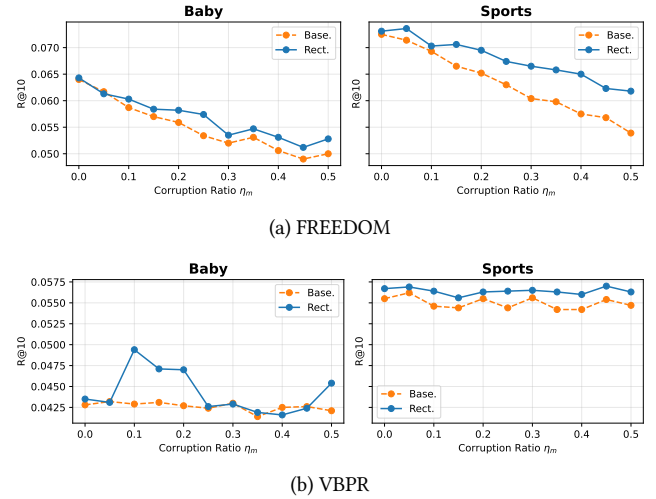


**Figure 2: Robustness under modality misalignment.** Recall@10 of FREEDOM and VBPR on Baby and Sports as the modality corruption ratio  $\eta_m$  increases. **BASE.** denotes the original backbone using corrupted features, and **RECT.** applies our Modality-level Rectification as offline preprocessing.

MR can suppress subtle mismatches while preserving the original signals, making it a safe preprocessing step for downstream recommenders.

**Practical note on memory.** For LATTICE on Electronics, we observe CUDA out-of-memory (OOM) under our fixed experimental setting when keeping the backbone and hyperparameters unchanged. We therefore omit these results and focus on the remaining backbones, where MR can be applied efficiently and consistently.

## 6.3 Modality-level Rectification: Robustness Under Modality Corruption

We evaluate the robustness of the proposed Modality-level Rectification under feature-level untrustworthiness by progressively increasing the modality-misalignment ratio  $\eta_m$  from 0 to 0.5. Following the corruption protocol in Sec. 3, we independently permute a fraction of image/text features and report Recall@10 on two datasets (Baby and Sports). Figure 2 compares the vanilla backbones (BASE.) and their rectified counterparts (RECT.) on a graph-based multimodal model (FREEDOM) and an MF-style model (VBPR).

**Overall robustness gains across model families.** As shown in Figure 2, rectification consistently improves robustness on both the graph-based backbone (FREEDOM) and the MF-style backbone (VBPR) across datasets and noise levels. The improvement becomes more evident as  $\eta_m$  increases, indicating that learning soft item-modality correspondences effectively mitigates the impact of modality misalignment on downstream preference learning.

**Table 2: Clean performance on Baby, Sports, and Electronics.** MR denotes our Modality-level Rectification applied as offline preprocessing by replacing modality inputs. We report Recall@10/20 and NDCG@10/20; the better result between the backbone and +MR is **bolded**. OOM indicates CUDA out-of-memory under this fixed setting.

Dataset	Metric	MF-based model				GNN-based model					
		VBPR	+MR	LATTICE	+MR	MGCN	+MR	FREEDOM	+MR	SMORE	+MR
Baby	R@10	0.0428	0.0428	0.0537	<b>0.0562</b>	0.0613	<b>0.0627</b>	0.0624	<b>0.0641</b>	0.0647	<b>0.0684</b>
	R@20	<b>0.0665</b>	0.0658	0.0837	<b>0.0852</b>	0.0939	<b>0.0946</b>	0.0977	<b>0.1001</b>	0.1007	<b>0.1037</b>
	N@10	0.0226	<b>0.0231</b>	0.0289	<b>0.0301</b>	0.0328	<b>0.0343</b>	0.0326	<b>0.0341</b>	0.0355	<b>0.0379</b>
	N@20	0.0287	<b>0.0291</b>	0.0366	<b>0.0376</b>	0.0412	<b>0.0425</b>	0.0417	<b>0.0433</b>	0.0448	<b>0.0469</b>
Sports	R@10	0.0550	<b>0.0571</b>	<b>0.0625</b>	0.0617	<b>0.0713</b>	0.0712	0.0717	<b>0.0730</b>	0.0736	<b>0.0738</b>
	R@20	0.0841	<b>0.0879</b>	<b>0.0954</b>	0.0912	<b>0.1060</b>	0.1056	0.1088	<b>0.1114</b>	0.1105	<b>0.1110</b>
	N@10	0.0300	<b>0.0308</b>	<b>0.0337</b>	0.0334	0.0385	0.0385	0.0389	<b>0.0397</b>	<b>0.0405</b>	0.0402
	N@20	0.0375	<b>0.0387</b>	<b>0.0423</b>	0.0410	<b>0.0475</b>	0.0474	0.0485	<b>0.0496</b>	<b>0.0500</b>	0.0498
Electronics	R@10	0.0281	<b>0.0299</b>	OOM	OOM	0.0418	0.0418	0.0377	<b>0.0397</b>	0.0400	<b>0.0437</b>
	R@20	0.0434	<b>0.0465</b>	OOM	OOM	0.0619	0.0619	0.0577	<b>0.0602</b>	0.0648	<b>0.0650</b>
	N@10	0.0152	<b>0.0161</b>	OOM	OOM	0.0234	0.0234	0.0207	<b>0.0218</b>	<b>0.0247</b>	0.0244
	N@20	0.0192	<b>0.0204</b>	OOM	OOM	0.0287	0.0287	0.0259	<b>0.0271</b>	<b>0.0301</b>	0.0299

*Why FREEDOM benefits more under modality mismatch.* FREEDOM exhibits a clear performance degradation as  $\eta_m$  grows, especially on Sports, whereas the rectified version maintains substantially higher Recall@10. This is expected because FREEDOM leverages modality features to construct modality-induced item-item relations; once modality features are mismatched, the induced item-item graph can introduce erroneous neighbors and amplify unreliable signals through message passing, leading to sharper performance drops. By rectifying item-side modality features before they are used to form such relations, our module reduces the chance of constructing misleading item-item connections, hence improving robustness.

*VBPR is intrinsically more robust, yet still benefits from rectification.* In contrast, VBPR is relatively insensitive to modality misalignment: its performance curves are much flatter across  $\eta_m$ . A plausible reason is that VBPR incorporates multimodal features as an additive preference term in an MF-style scoring function; when modality information becomes unreliable, the model can rely more on the collaborative (ID) component, thus maintaining performance. Nevertheless, rectification still brings consistent gains, and on Baby we observe a notable improvement around  $\eta_m \approx 0.1-0.2$ . We conjecture that the soft rectification can partially absorb corrupted modality signals, making the residual modality input less misleading and yielding an effect akin to “noise injection + denoised reconstruction”, which helps VBPR extract more useful content information in this regime.

Overall, these results demonstrate that the proposed rectification serves as a robust, plug-and-play preprocessing module that improves multimodal recommendation under modality misalignment, benefiting both graph-based and MF-style backbones.

#### 6.4 Hyperparameter Sensitivity

We study the sensitivity of Modality-level Rectification to two key hyperparameters: the diagonal prior mix ratio  $\lambda$  in Eq. (13) and the

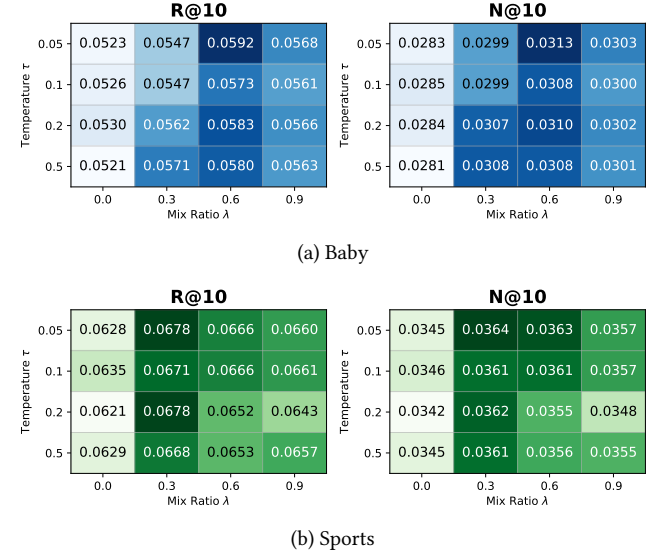


**Figure 3: Hyperparameter sensitivity of MR under modality corruption ( $\eta_m = 0.2$ ) on FREEDOM.** We vary the mix ratio  $\lambda$  and temperature  $\tau$ , and report Recall@10 and NDCG@10 on Baby and Sports.

temperature  $\tau$  in the affinity construction (Eq. (10)). To highlight the effect under feature-level untrustworthiness, we conduct experiments with a fixed modality corruption ratio  $\eta_m = 20\%$  and evaluate FREEDOM on Baby and Sports using Recall@10 and NDCG@10.

Figure 3 shows that intermediate mixing generally yields the best performance. Across both datasets and metrics, the sweet spot lies around  $\lambda \approx 0.6$ , suggesting that a conservative rectification is beneficial: fully replacing the observed features ( $\lambda = 0$ ) can be too aggressive, while relying almost entirely on the corrupted

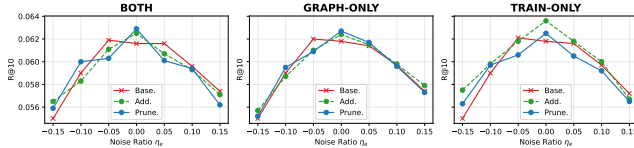


**Figure 4: Interaction-level stress test on Baby with MGCN.** We report Recall@10 as the interaction noise ratio  $\eta_e$  varies. **BASE.** is the original backbone; **ADD.** and **PRUNE.** apply similarity-based relation completion or edge pruning using a LightGCN prior. **TRAIN-ONLY** edits BPR positives, **GRAPH-ONLY** edits the propagation graph, and **BOTH** edits both supervision and propagation.

observation ( $\lambda \rightarrow 1$ ) weakens the correction effect. Overall, MR is relatively robust to  $\lambda$  within a broad mid-range (roughly 0.3–0.6), while extreme values tend to be suboptimal.

The temperature  $\tau$  controls the sharpness of the sparse affinity weights before Sinkhorn scaling. We observe that MR is stable across a reasonable range of  $\tau$ , with  $\tau$  in the lower-to-mid regime (e.g., 0.05–0.2) typically performing well. Very large temperatures (e.g.,  $\tau = 0.5$ ) make affinities overly smooth, which may dilute the correspondence signal and slightly reduce performance.

In summary, MR is stable w.r.t. both hyperparameters under modality corruption; we use  $\lambda = 0.5$  as a stable default within the broad optimal region and set  $\tau = 0.1$  in all experiments. We further provide an ablation study in Appendix A, verifying the contribution of Sinkhorn balancing and small-loss projection.

## 6.5 Interaction-level Insight Results

We empirically validate our interaction-level insights by stress-testing a collaborative-prior-based edge editing pipeline on a graph-based multimodal recommender. Specifically, we report Recall@10 of MGCN on the Baby dataset under interaction noise ratios  $\eta_e \in [-0.15, 0.15]$  (Sec. 3), where negative values correspond to random edge deletions and positive values correspond to random edge additions in the training interactions. We compare the vanilla backbone (BASE.) with two similarity-based editing operations derived from a LightGCN prior: ADD. (relation completion) and PRUNE. (edge pruning). We further evaluate three ways to apply the edits: TRAIN-ONLY (edit BPR positives), GRAPH-ONLY (edit the propagation graph), and BOTH (edit both supervision and propagation).

*No-noise regime: prior-based completion/pruning is beneficial.* As shown in Figure 4, when there is no interaction noise ( $\eta_e = 0$ ), both ADD. and PRUNE. consistently outperform the base model across all three application choices. This indicates that, when the observed training interactions are reliable, the LightGCN prior provides a meaningful similarity signal  $s_{ui}$  and similarity-based edge editing can refine neighborhoods and improve learning.

*Under stress tests: the effect becomes unstable and can backfire.* Once interaction noise is injected, the benefit of edge editing becomes non-monotonic and depends on the noise type and the alignment between the learned prior and the true preference signal. Under random edge additions ( $\eta_e > 0$ ), the collaborative prior is more likely to be contaminated by spurious positives; as a result,

the gains of ADD./PRUNE. diminish and can even disappear, making the base model competitive or preferable in some settings. Under random edge deletions ( $\eta_e < 0$ ), the prior can sometimes help recover useful structure, but can also become misleading when missing edges distort neighborhood information, leading to mixed outcomes.

*Train-only vs. graph-only vs. both.* Across noise levels, TRAIN-ONLY editing tends to be more volatile since it directly performs label editing on BPR positives and thus perturbs the supervision signal. GRAPH-ONLY editing isolates the intervention to message passing and can be more stable, yet it may still amplify misaligned neighbors when the prior is noisy. Applying edits to BOTH can compound these effects: it simultaneously changes the supervision signal and the propagation neighborhood, which can magnify the impact of prior contamination under interaction noise.

Overall, Figure 4 confirms that collaborative-prior-based edge editing is not a universal remedy for noisy implicit feedback: it is reliably beneficial in clean graphs but can become unstable and even harmful under stress tests, motivating careful validation and conservative usage in practice.

## 7 Conclusion

This work studies trustworthiness in multimodal recommender systems (MRSs) from both content and interaction perspectives. We propose a plug-and-play modality-level rectification module that mitigates untrustworthy multimodal features (e.g., mismatched images or misleading text) via lightweight projection and Sinkhorn-based soft matching, suppressing mismatched signals while preserving consistent semantics.

We further conduct controlled stress tests on interaction-level trustworthiness and show that collaborative-prior-based graph editing (similarity-based completion and pruning) is not universally beneficial: it is typically helpful when interactions are clean, but becomes non-monotonic under interaction corruption, helping or hurting depending on noise type and the alignment (reliability) of the learned prior. Moreover, editing the propagation graph may amplify misaligned relations via message passing, while editing supervision perturbs the learning signal, highlighting the need for careful validation before deployment.

Our study focuses on image/text modalities and specific corruption patterns; future work may extend to additional modalities and more realistic trustworthiness failures. Designing principled, alignment-aware mechanisms for graph editing and propagation under untrustworthy interactions also remains an important direction. Extensive experiments across datasets and backbones demonstrate the robustness gains from rectification and support our interaction-level findings, and we will release code and data to facilitate further research.

## References

- [1] G. Adomavicius and A. Tuzhilin. 2005. Toward the next Generation of Recommender Systems: A Survey of the State-of-the-Art and Possible Extensions. *IEEE Transactions on Knowledge and Data Engineering* 17, 6 (June 2005), 734–749. doi:10.1109/TKDE.2005.99
- [2] Feiyu Chen, Junjie Wang, Yinwei Wei, Hai-Tao Zheng, and Jie Shao. 2022. Breaking Isolation: Multimodal Graph Fusion for Multimedia Recommendation by Edge-wise Modulation. In *Proceedings of the 30th ACM International Conference*

on *Multimedia (MM '22)*. Association for Computing Machinery, New York, NY, USA, 385–394. doi:10.1145/3503161.3548399

[3] Zefeng Chen, Wensheng Gan, Jiayang Wu, Kaixia Hu, and Hong Lin. 2023. Data Scarcity in Recommendation Systems: A Survey. arXiv:2312.10073 [cs] doi:10.48550/arXiv.2312.10073

[4] Ching-Yao Chuang, R. Devon Hjelm, Xin Wang, Vibhav Vineet, Neel Joshi, Antonio Torralba, Stefanie Jegelka, and Yale Song. 2022. Robust Contrastive Learning against Noisy Views. arXiv:2201.04309 [cs] doi:10.48550/arXiv.2201.04309

[5] Ziwei Fan, Ke Xu, Zhang Dong, Hao Peng, Jiawei Zhang, and Philip S. Yu. 2023. Graph Collaborative Signals Denoising and Augmentation for Recommendation. arXiv:2304.03344 [cs] doi:10.48550/arXiv.2304.03344

[6] Ruining He and Julian McAuley. 2015. VBPR: Visual Bayesian Personalized Ranking from Implicit Feedback. arXiv:1510.01784 [cs] doi:10.48550/arXiv.1510.01784

[7] Xiangnan He, Kuan Deng, Xiang Wang, Yan Li, Yongdong Zhang, and Meng Wang. 2020. LightGCN: Simplifying and Powering Graph Convolution Network for Recommendation. arXiv:2002.02126 [cs] doi:10.48550/arXiv.2002.02126

[8] Zhenyu Huang, Guocheng Niu, Xiao Liu, Wenbiao Ding, Xinyan Xiao, Hua Wu, and Xi Peng. [n. d.]. Learning with Noisy Correspondence for Cross-modal Matching. ([n. d.]).

[9] Wang-Cheng Kang, Chen Fang, Zhaowen Wang, and Julian McAuley. 2017. Visually-Aware Fashion Recommendation and Design with Generative Image Models. arXiv:1711.02231 [cs] doi:10.48550/arXiv.1711.02231

[10] Xuan Nhat Lam, Thuc Vu, Trong Duc Le, and Anh Duc Duong. 2008. Addressing Cold-Start Problem in Recommendation Systems. In *Proceedings of the 2nd International Conference on Ubiquitous Information Management and Communication (ICUIMC '08)*. Association for Computing Machinery, New York, NY, USA, 208–211. doi:10.1145/1352793.1352837

[11] Qidong Liu, Jiaxi Hu, Yutian Xiao, Xiangyu Zhao, Jingtong Gao, Wanyu Wang, Qing Li, and Jiliang Tang. 2024. Multimodal Recommender Systems: A Survey. arXiv:2302.03883 [cs] doi:10.48550/arXiv.2302.03883

[12] Rongqing Kenneth Ong and Andy W. H. Khong. 2025. Spectrum-Based Modality Representation Fusion Graph Convolutional Network for Multimodal Recommendation. In *Proceedings of the Eighteenth ACM International Conference on Web Search and Data Mining*. 773–781. arXiv:2412.14978 [cs] doi:10.1145/3701551.3703561

[13] Nils Reimers and Iryna Gurevych. 2019. Sentence-BERT: Sentence Embeddings Using Siamese BERT-Networks. arXiv:1908.10084 [cs] doi:10.48550/arXiv.1908.10084

[14] Steffen Rendle, Christoph Freudenthaler, Zeno Gantner, and Lars Schmidt-Thieme. 2012. BPR: Bayesian Personalized Ranking from Implicit Feedback. arXiv:1205.2618 [cs] doi:10.48550/arXiv.1205.2618

[15] Paul Resnick, Neophyots Iacovou, Mitesh Suchak, Peter Bergstrom, and John Riedl. 1994. GroupLens: An Open Architecture for Collaborative Filtering of Netnews. In *Proceedings of the 1994 ACM Conference on Computer Supported Cooperative Work (CSCW '94)*. Association for Computing Machinery, New York, NY, USA, 175–186. doi:10.1145/192844.192905

[16] Francesco Ricci, Lior Rokach, and Bracha Shapira (Eds.). 2022. *Recommender Systems Handbook*. Springer US, New York, NY. doi:10.1007/978-1-0716-2197-4

[17] J. Ben Schafer, Joseph A. Konstan, and John Riedl. 2001. E-Commerce Recommendation Applications. *Data Mining and Knowledge Discovery* 5, 1 (Jan. 2001), 115–153. doi:10.1023/A:1009804230409

[18] Andrew I. Schein, Alexandrin Popescul, Lyle H. Ungar, and David M. Pennock. 2002. Methods and Metrics for Cold-Start Recommendations. In *Proceedings of the 25th Annual International ACM SIGIR Conference on Research and Development in Information Retrieval (SIGIR '02)*. Association for Computing Machinery, New York, NY, USA, 253–260. doi:10.1145/564376.564421

[19] Karen Simonyan and Andrew Zisserman. 2015. Very Deep Convolutional Networks for Large-Scale Image Recognition. arXiv:1409.1556 [cs] doi:10.48550/arXiv.1409.1556

[20] Zhulin Tao, Xiaohao Liu, Yewei Xia, Xiang Wang, Lifang Yang, Xianglin Huang, and Tat-Seng Chua. 2023. Self-Supervised Learning for Multimedia Recommendation. *IEEE Transactions on Multimedia* 25 (2023), 5107–5116. doi:10.1109/TMM.2022.3187556

[21] Ivona Tautkute, Tomasz Trzcinski, Aleksander Skorupa, Lukasz Brocki, and Krzysztof Marasek. 2019. DeepStyle: Multimodal Search Engine for Fashion and Interior Design. arXiv:1801.03002 [cs] doi:10.48550/arXiv.1801.03002

[22] Qifan Wang, Yinwei Wei, Jianhua Yin, Jianlong Wu, Xuemeng Song, and Liqiang Nie. 2023. DualGNN: Dual Graph Neural Network for Multimedia Recommendation. *IEEE Transactions on Multimedia* 25 (2023), 1074–1084. doi:10.1109/TMM.2021.3138298

[23] Wenjie Wang, Fuli Feng, Xiangnan He, Liqiang Nie, and Tat-Seng Chua. 2021. Denoising Implicit Feedback for Recommendation. In *Proceedings of the 14th ACM International Conference on Web Search and Data Mining*. 373–381. arXiv:2006.04153 [cs] doi:10.1145/3437963.3441800

[24] Xiang Wang, Xiangnan He, Meng Wang, Fuli Feng, and Tat-Seng Chua. 2019. Neural Graph Collaborative Filtering. In *Proceedings of the 42nd International ACM SIGIR Conference on Research and Development in Information Retrieval*. 165–174. arXiv:1905.08108 [cs] doi:10.1145/3331184.3331267

[25] Yinwei Wei, Xiang Wang, Liqiang Nie, Xiangnan He, Richang Hong, and Tat-Seng Chua. 2019. MMGCN: Multi-modal Graph Convolution Network for Personalized Recommendation of Micro-video. In *Proceedings of the 27th ACM International Conference on Multimedia (MM '19)*. Association for Computing Machinery, New York, NY, USA, 1437–1445. doi:10.1145/3343031.3351034

[26] Guipeng Xv, Xinyu Li, Ruobing Xie, Chen Lin, Chong Liu, Feng Xia, Zhanhui Kang, and Leyu Lin. 2024. Improving Multi-modal Recommender Systems by Denoising and Aligning Multi-modal Content and User Feedback. In *Proceedings of the 30th ACM SIGKDD Conference on Knowledge Discovery and Data Mining (KDD '24)*. Association for Computing Machinery, New York, NY, USA, 3645–3656. doi:10.1145/3637528.3671703

[27] Mouxing Yang, Yunfan Li, Zhenyu Huang, Zitao Liu, Peng Hu, and Xi Peng. 2021. Partially View-aligned Representation Learning with Noise-robust Contrastive Loss. In *2021 IEEE/CVF Conference on Computer Vision and Pattern Recognition (CVPR)*. IEEE, Nashville, TN, USA, 1134–1143. doi:10.1109/CVPR46437.2021.00119

[28] Shuo Yang, Zhaopan Xu, Kai Wang, Yang You, Hongxun Yao, Tongliang Liu, and Min Xu. 2023. BiCro: Noisy Correspondence Rectification for Multi-modality Data via Bi-directional Cross-modal Similarity Consistency. arXiv:2303.12419 [cs] doi:10.48550/arXiv.2303.12419

[29] Yuchen Yang, Likai Wang, Erkun Yang, and Cheng Deng. 2024. Robust Noisy Correspondence Learning with Equivariant Similarity Consistency. In *2024 IEEE/CVF Conference on Computer Vision and Pattern Recognition (CVPR)*. IEEE, Seattle, WA, USA, 17700–17709. doi:10.1109/CVPR52733.2024.01676

[30] Rex Ying, Ruining He, Kaifeng Chen, Pong Eksombatchai, William L. Hamilton, and Jure Leskovec. 2018. Graph Convolutional Neural Networks for Web-Scale Recommender Systems. In *Proceedings of the 24th ACM SIGKDD International Conference on Knowledge Discovery & Data Mining*. 974–983. arXiv:1806.01973 [cs] doi:10.1145/3219819.3219890

[31] Wei Yinwei, Wang Xiang, Nie Liqiang, He Xiangnan, and Chua Tat-Seng. 2021. GRCN: Graph-Refined Convolutional Network for Multimedia Recommendation with Implicit Feedback. arXiv:2111.02036 [cs] doi:10.48550/arXiv.2111.02036

[32] Penghang Yu, Zhiyi Tan, Guanming Lu, and Bing-Kun Bao. 2023. Multi-View Graph Convolutional Network for Multimedia Recommendation. In *Proceedings of the 31st ACM International Conference on Multimedia*. 6576–6585. arXiv:2308.03584 [cs] doi:10.1145/3581783.3613915

[33] Penghang Yu, Zhiyi Tan, Guanming Lu, and Bing-Kun Bao. 2025. Mind Individual Information! Principal Graph Learning for Multimedia Recommendation. *Proceedings of the AAAI Conference on Artificial Intelligence* 39, 12 (April 2025), 13096–13105. doi:10.1609/aaai.v39i12.33429

[34] Jinghai Zhang, Yanqiao Zhu, Qiang Liu, Shu Wu, Shuhui Wang, and Liang Wang. 2021. Mining Latent Structures for Multimedia Recommendation. In *Proceedings of the 29th ACM International Conference on Multimedia*. 3872–3880. arXiv:2104.09036 [cs] doi:10.1145/3474085.3475259

[35] Hongyu Zhou, Xin Zhou, Zhiwei Zeng, Lingzi Zhang, and Zhiqi Shen. 2023. A Comprehensive Survey on Multimodal Recommender Systems: Taxonomy, Evaluation, and Future Directions. arXiv:2302.04473 [cs] doi:10.48550/arXiv.2302.04473

[36] Hongyu Zhou, Xin Zhou, Lingzi Zhang, and Zhiqi Shen. 2023. Enhancing Dyadic Relations with Homogeneous Graphs for Multimodal Recommendation. arXiv:2301.12097 [cs] doi:10.48550/arXiv.2301.12097

[37] Xin Zhou. 2023. MMRec: Simplifying Multimodal Recommendation. In *ACM Multimedia Asia Workshops*. 1–2. arXiv:2302.03497 [cs] doi:10.1145/3611380.3628561

[38] Xin Zhou and Zhiqi Shen. 2023. A Tale of Two Graphs: Freezing and Denoising Graph Structures for Multimodal Recommendation. In *Proceedings of the 31st ACM International Conference on Multimedia*. 935–943. arXiv:2211.06924 [cs] doi:10.1145/3581783.3611943

[39] Xin Zhou, Hongyu Zhou, Yong Liu, Zhiwei Zeng, Chunyan Miao, Pengwei Wang, Yuan You, and Feijun Jiang. 2023. Bootstrap Latent Representations for Multi-modal Recommendation. In *Proceedings of the ACM Web Conference 2023 (WWW '23)*. Association for Computing Machinery, New York, NY, USA, 845–854. doi:10.1145/3543507.3583251

## A Modality-level Rectification: Ablation Study

We provide a lightweight ablation study to verify the necessity of key components in Modality-level Rectification (MR). Following the modality-corruption protocol in Sec. 3, we set the misalignment ratio to  $\eta_m = 20\%$  and evaluate FREEDOM on Baby and Sports using Recall@10 and NDCG@10.

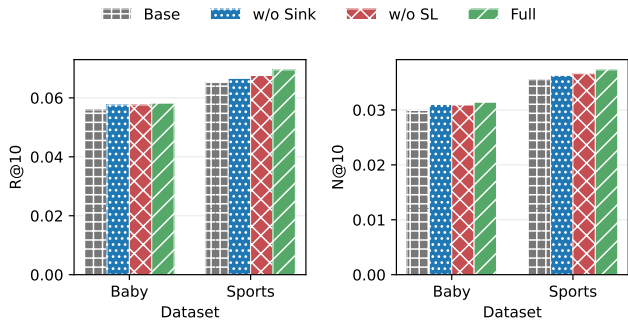


**Figure 5: Ablation study of MR under modality misalignment ( $\eta_m = 20\%$ ) with FREEDOM on Baby and Sports. We report Recall@10 and NDCG@10. **BASE**: w/o MR; **FULL**: full MR; **w/o SINK**: replace Sinkhorn matching with row-normalized affinity; **w/o SL**: remove small-loss selection in projection training.**

*Compared variants.* We consider four variants: (BASE) w/o MR, directly using the corrupted modality features; (FULL) the complete MR module; (w/o SINK) replacing Sinkhorn-based balancing with simple row normalization (row-norm) on the sparse affinity; (w/o SL) removing the small-loss selection strategy and training the projection with the full-batch loss.

*Results and analysis.* As shown in Figure 5, FULL achieves the best performance on both datasets and both metrics, confirming that MR is effective under modality misalignment. Both w/o SINK and w/o SL lead to consistent drops compared with FULL, indicating that (i) Sinkhorn balancing is helpful for mitigating hubness and producing more stable correspondences, and (ii) robust projection with small-loss selection improves alignment under mismatched item-modality pairs. Finally, BASE performs the worst, highlighting the severity of modality corruption and the necessity of rectification. Overall, the ablation supports that the proposed design components are complementary and jointly contribute to robustness.